Statistics of Complex Wigner Time Delays as a Counter of S-Matrix Poles: Theory and Experiment

Lei Chen,[1,2,*] Steven M. Anlage,[1,2,†] and Yan V. Fyodorov[3,4,‡]
[1]Quantum Materials Center, Department of Physics, University of Maryland, College Park, Maryland 20742, USA
[2]Department of Electrical and Computer Engineering, University of Maryland, College Park, Maryland 20742, USA
[3]Department of Mathematics, Kings College London, London WC26 2LS, United Kingdom
[4]L. D. Landau Institute for Theoretical Physics, Semenova 1a, 142432 Chernogolovka, Russia

(Received 25 June 2021; accepted 15 October 2021; published 12 November 2021)

We study the statistical properties of the complex generalization of Wigner time delay τ_{W} for subunitary wave-chaotic scattering systems. We first demonstrate theoretically that the mean value of the $\mathrm{Re}[\tau_W]$ distribution function for a system with uniform absorption strength η is equal to the fraction of scattering matrix poles with imaginary parts exceeding η. The theory is tested experimentally with an ensemble of microwave graphs with either one or two scattering channels and showing broken time-reversal invariance and variable uniform attenuation. The experimental results are in excellent agreement with the developed theory. The tails of the distributions of both real and imaginary time delay are measured and are also found to agree with theory. The results are applicable to any practical realization of a wave-chaotic scattering system in the short-wavelength limit, including quantum wires and dots, acoustic and electromagnetic resonators, and quantum graphs.

DOI: 10.1103/PhysRevLett.127.204101

Introduction.—In this Letter we are concerned with the general scattering properties of complex systems, namely finite-size wave systems with one or more channels connected to asymptotic states outside of the scattering domain. The scattering system is complex in the sense that classical ray trajectories will undergo chaotic scattering when propagating inside the closed system. We focus on the properties of the energy-dependent scattering matrix of the system, defined via the linear relationship between the outgoing $|\psi_{\mathrm{out}}\rangle$ and incoming wave amplitudes $|\psi_{\mathrm{in}}\rangle$ on the M coupled channels as $|\psi_{\mathrm{out}}\rangle = S|\psi_{\mathrm{in}}\rangle$. In the short-wavelength limit the complex $M \times M$ scattering matrix $S(E)$ is a strongly fluctuating function of energy E (or, equivalently, the frequency ω) of the incoming waves, as well as specific system details. Those parts of the fluctuations that reflect long-time behavior are controlled by the high density of S-matrix poles, or resonances, having their origin at eigenfrequencies (modes) of closed counterparts of the scattering systems. At energy scales comparable to the mean separation Δ between the neighboring eigenfrequencies, the properties of the scattering matrix are largely universal and depend on very few system-specific parameters. The ensuing statistical characteristics of the S-matrix have been very successfully studied theoretically over the past 3 decades using methods of random matrix theory (RMT) [1–9].

The scattering matrix can be characterized by the distribution of poles and associated zeros in the complex energy plane, which are most clearly seen when one addresses its determinant. In the unitary (zero loss) limit, the poles and zeros of the determinant form complex conjugate pairs across the real axis in the energy plane. In the presence of any loss, the poles and zeros are no longer complex conjugates, but if the loss is spatially uniform their positions are still simply related by a uniform shift. This is no longer the case for spatially localized losses, with poles and zeros migrating in a complicated way to new locations, subject to certain constraints. For a passive lossy system the poles always remain in the lower half of the complex energy plane, while the zeros can freely move between the two sides of the real axis. Among other things, rising recent interest in characterizing S-matrix complex zeros, as well as their manifestation in physical observables, is strongly motivated by the phenomenon of coherent perfect absorption [10], see [11–15] and references therein.

One quantity that is closely related to resonances is known to be the Wigner time delay τ_W. In its traditional definition [16,17] for unitary, flux conserving scattering systems the Wigner time delay τ_W is a real positive quantity measuring how long an excitation lingers in the scattering region before leaving through one of the M channels. Fluctuations of τ_W and related quantities was the subject of a large number of theoretical works in the RMT context [18–27], and more recently [28–32], as well in a semiclassical context in [33–36] and references therein. In particular, for the one- and two-channel cases most relevant to this Letter the distribution of τ_W is known explicitly for all symmetry classes, $\beta = 1$, 2, and 4 [24].

Experimental work on time delays in wave-chaotic billiard systems was pioneered by Doron, Smilansky, and Frenkel in microwave billiards with uniform absorption [37],

where the relation between the Wigner time delays and the unitary deficit of the S-matrix was explored. Later experiments on time delay statistics were made by Genack and coworkers, who studied microwave pulse delay times through randomized dielectric scatterers [38,39]. The quantity studied in that case is a type of partial time delay associated with the complex transmission amplitude between channels [40], somewhat different from the Wigner time delay. In particular, contributions to the transmission time delay due to poles and zeros of the off-diagonal S-matrix entries have been identified [41].

Despite strong interest in the standard Wigner time delay over the years, its use for characterizing statistics of S-matrix poles and zeros beyond the regime of well-resolved (isolated) resonances has been always problematic. In our recent article [15] we noticed that in the presence of losses one may propose a complex-valued generalization of the Wigner time delay τ_W (CWTD) that reflects the phase and amplitude variation of the scattering matrix with energy. Subsequently, we developed a method, both experimentally and theoretically, for exploiting CWTD for identifying the locations of individual S-matrix poles $\mathcal{E}_n$ and zeros z_n in the complex energy plane. The method has been implemented in the regime of well-resolved, isolated resonances, for systems with both localized and uniform sources of absorption. However, no statistical characterization of CWTD for large numbers of modes has been attempted.

To this end it is worth mentioning that one of the oldest yet useful facts about the standard Wigner time delay is that the mean of the τ_W distribution is simply related to the Heisenberg time τ_H of the system, $\langle \tau_W \rangle = 2\pi\hbar/M\Delta := \tau_H/M$ [42]. As such it is absolutely insensitive to the type of dynamics, chaotic vs integrable. More recently this property was put in a much wider context and tested experimentally [43].

In this Letter we reveal that the mean value of $\mathrm{Re}[\tau_W]$ of CWTD is, in striking contrast to the flux-conserving case, a much richer object and can be used to obtain nontrivial information about the distribution of the imaginary part of the poles of the S-matrix. For this we develop the corresponding theory for the mean values and compare to the experimentally observed evolution of distributions of real and imaginary parts of CWTD with uniform loss variation.

Theory.—The appropriate theoretical framework for our analysis is the so-called effective Hamiltonian formalism for wave-chaotic scattering [3,4,7,9,44]. It starts with defining an $N \times N$ self-adjoint matrix Hamiltonian H whose real eigenvalues are associated with eigenfrequencies of the closed system. Further defining W to be an $N \times M$ matrix of coupling elements between the N modes of H and the M scattering channels, one can in the standard way build the unitary $M \times M$ scattering matrix $S(E)$. In this approach the S-matrix poles $\mathcal{E}_n = E_n - i\Gamma_n$ (with $\Gamma_n > 0$) are complex eigenvalues of the non-Hermitian effective Hamiltonian matrix $\mathcal{H}_{\mathrm{eff}} = H - i\Gamma_W \neq \mathcal{H}_{\mathrm{eff}}^{\dagger}$, where we defined $\Gamma_W = \pi W W^{\dagger}$. A standard way of incorporating the uniform absorption with strength η is to replace $E \to E + i\eta$ making S-matrix subunitary, such that its determinant $\det S(E + i\eta)$ is given by the ratio

$$\frac{\det[E - H + i(\eta - \Gamma_W)]}{\det[E - H + i(\eta + \Gamma_W)]} = \prod_{n=1}^{N} \frac{E + i\eta - \mathcal{E}_n^*}{E + i\eta - \mathcal{E}_n}, \tag{1}$$

Using the above expression, the Wigner time delay can be very naturally extended to scattering systems with uniform absorption as suggested in [15] by defining

$$\tau_W(E;\eta) := \frac{-i}{M}\frac{\partial}{\partial E}\log\det S(E + i\eta) = \mathrm{Re}\tau_W(E;\eta) + i\mathrm{Im}\tau_W(E;\eta), \tag{2}$$

$$\mathrm{Re}\tau_W(E;\eta) = \frac{1}{M}\sum_{n=1}^{N}\left[\frac{\Gamma_n + \eta}{(E - E_n)^2 + (\Gamma_n + \eta)^2} - \frac{\eta - \Gamma_n}{(E - E_n)^2 + (\Gamma_n - \eta)^2}\right], \tag{3}$$

$$\mathrm{Im}\tau_W(E;\eta) = -\frac{1}{M}\sum_{n=1}^{N}\left[\frac{4\eta\Gamma_n(E - E_n)}{[(E - E_n)^2 + (\Gamma_n - \eta)^2][(E - E_n)^2 + (\Gamma_n + \eta)^2]}\right]. \tag{4}$$

For a wave-chaotic system the set of parameters Γ_n, E_n (known as the *resonance widths* and *positions*, respectively) is generically random. Namely, even minute changes in microscopic shape characteristics of the system will drastically change the particular arrangement of S-matrix poles in the complex plane in systems that are otherwise macroscopically indistinguishable. To study the associated statistics of CWTD most efficiently one may invoke the notion of an *ensemble* of such systems. As a result, both $\mathrm{Re}[\tau_W]$ and $\mathrm{Im}[\tau_W]$ at a given energy will be distributed over a wide range of values. Alternatively, even in a single wave-chaotic system the CWTD will display considerable statistical fluctuations when sampled over an ensemble of different *mesoscopic* energy intervals; see below and the Supplemental Material [45] for more detailed discussion. Invoking the notion of spectral ergodicity, one expects that

in wave-chaotic systems the two types of ensembles (i.e., those produced by perturbations to the system at fixed energy vs those created by considering various energy windows) should be equivalent.

Consider the mean value of the CWTD in systems with uniform absorption $\eta > 0$. In contrast to the case of flux-conserving systems the mean of $\mathrm{Re}[\tau_W]$ becomes highly nontrivial as it counts the number of S-matrix poles whose widths exceed the uniform absorption strength value. In other words,

$$\frac{\langle \mathrm{Re}[\tau_W(E;\eta)]\rangle_E}{\tau_H/M} = \frac{\text{no.of}[\Gamma_n > \eta \text{ such that } E_n \text{ is inside } I_E]}{\text{total no. of resonances inside } I_E}, \tag{5}$$

where I_E is a mesoscopic energy interval that is much larger than the mean mode spacing Δ, absorption η, and the widths Γ_n, but small enough so that the interval has a roughly constant mode density. To prove this, perform an energy average of Eq. (3):

$$\begin{aligned}
&\langle \mathrm{Re}[\tau_W(E;\eta)]\rangle_E \\
&\approx \frac{\pi/2}{M|I|}\sum_{n=1}^{N}\left\{\left[\mathrm{sign}\left(\frac{E_R-E_n}{\eta+\Gamma_n}\right)-\mathrm{sign}\left(\frac{E_L-E_n}{\eta+\Gamma_n}\right)\right]\right. \\
&\quad \left.-\left[\mathrm{sign}\left(\frac{E_R-E_n}{\eta-\Gamma_n}\right)-\mathrm{sign}\left(\frac{E_L-E_n}{\eta-\Gamma_n}\right)\right]\right\} \\
&= \frac{2\pi}{M|I|}\sum_{n=1}^{N}\theta(\Gamma_n-\eta),
\end{aligned} \tag{6}$$

where $|I| \coloneqq |E_R - E_L|$ is the mesoscopic energy interval and the step function $\theta(x) = 1$ for $x > 0$ and $\theta(x) = 0$ otherwise. Under the assumption that no. of $(E_n \in I) \approx |I|/\Delta$ we arrive at Eq. (5). Alternatively, invoking ergodicity, one may use the RMT for analyzing the mean CWTD, which independently confirms Eq. (5). Such analysis also predicts that $\langle \mathrm{Im}[\tau_W(E,\eta)\rangle_E = 0$, independent of η. Details of these calculations are presented in the Supplemental Material, Sec. I [45]. The distribution of imaginary parts Γ_n of the S-matrix poles relevant for Eq. (5) have been examined theoretically in the RMT framework [50–53] and experimentally [54–59] by a number of groups.

Experiment.—We test our theory by using an ensemble of tetrahedral microwave graphs with either $M = 1$ or $M = 2$ channels coupled to the outside world. We focus on experiments involving microwave graphs [60–63] for a number of reasons: one can precisely vary the uniform loss and the lumped loss over a wide range; one can work in either the time-reversal invariant (TRI) or broken TRI regimes; one can gather very good statistics with a large ensemble of graphs; and one can vary both the (energy-independent) mode density and loss to go from the limit of isolated modes to strongly overlapping modes. The disadvantages of graphs for statistical studies include significant reflections at nodes, which can create trapped modes on the bonds [64], and the appearance of short periodic orbits in cyclic graphs [65].

The microwave graphs are constructed with coaxial cables with center conductors of diameter 0.036 in. (0.92 mm) made with silver-plated copper-clad steel and outer shield of diameter 0.117 in. (2.98 mm) made with a copper-tin composite. An ensemble of microwave graphs is created by choosing six out of nine cables with different incommensurate lengths [for a total of $\binom{9}{6} = 84$ realizations] and creating uniquely different tetrahedral graphs. The scattering matrix of the one- and two-port graphs are measured with a calibrated Agilent PNA-X N5242A Network Analyzer (see insets of Fig. 3) over the frequency range from 1 to 12.4 GHz, which includes about 250 modes in a typical realization of the ensemble. The graphs are measured with a finite coupling strength g_a, which varies from 1.06 to 1.80 as a function of frequency, where $g_a = (2/T_a) - 1$ and $T_a = 1 - |S_{\mathrm{rad}}|^2$ is the transparency of the graph to the scattering channel a determined by the value of the radiation S-matrix. [66] The effects of the coupling are then removed through application of the random coupling model (RCM) normalization process [67–70]. This is equivalent to creating an ensemble of data with perfect coupling, $g_a = 1$ and $T_a = 1$ for all frequencies, ports, and realizations.

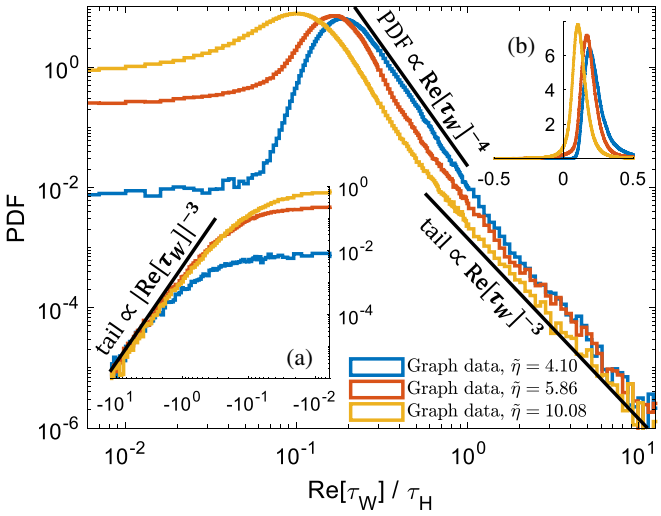

FIG. 1. Evolution of the PDF of measured $\mathrm{Re}[\tau_W]$ with increasing uniform attenuation ($\tilde{\eta}$) from an ensemble of two-port ($M = 2$) tetrahedral microwave graphs with broken TRI. The main figure and inset (a) show the distributions of the positive and negative $\mathrm{Re}[\tau_W]$ on a log-log scale for three values of uniform attenuation, respectively. Reference lines characterizing power-law behavior are added to the tails. Inset (b) shows the distributions of $\mathrm{Re}[\tau_W]$ on a linear scale for the same measured data.

TRI was broken in the graph by means of one of four different microwave circulators [71] operating in partially overlapping frequency ranges going from 1 to 12.4 GHz (see Supplemental Material, Sec. VI [45]). The CWTD τ_W is calculated using the RCM-normalized scattering matrix S as in Eq. (2), and the statistics of the real and imaginary parts are compiled based on realization averaging and frequency averaging in a given frequency band. The overall level of attenuation was varied by adding identical fixed microwave attenuators to each of the six bonds of the tetrahedral graphs [72]. The attenuator values chosen were 0.5, 1, and 2 dB.

Comparison of theory and experiments.—Our prior work showed that CWTD varied systematically as a function of energy or frequency for an isolated mode of a microwave graph [15]. The real and imaginary parts of τ_W take on both positive and negative values. We now consider an ensemble of graphs and examine the distribution of these values taken over many realizations and modes. We first examine the evolution of the probability density function (PDF) of $\mathrm{Re}[\tau_W]$ [Fig. 1(b)] and $\mathrm{Im}[\tau_W]$ (inset of Fig. 2) with increasing uniform (normalized) attenuation $\tilde{\eta}$. The uniform attenuation is quantified from the experiment as $\tilde{\eta} = (2\pi/\Delta)\eta = 4\pi\alpha$, where $\alpha = \delta f_{3\,\mathrm{dB}}/\Delta_f$, $\delta f_{3\,\mathrm{dB}}$ is the typical 3-dB bandwidth of the modes and Δ_f is the mean frequency spacing of the modes [73].

Figure 1 shows that as the uniform attenuation ($\tilde{\eta}$) of the graphs increases, the peak of the $\mathrm{Re}[\tau_W]$ distribution shifts to lower values. Furthermore, Fig. 1(a) shows that $\mathrm{Re}[\tau_W]$ acquires more negative values as the attenuation increases.

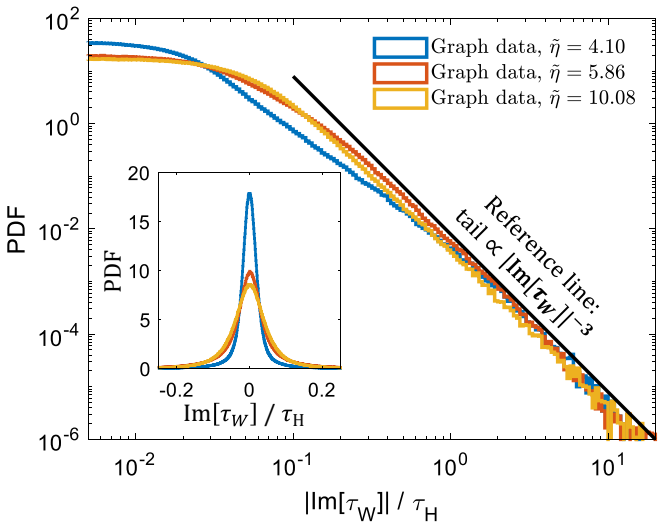

FIG. 2. Evolution of the PDF of measured $\mathrm{Im}[\tau_W]$ with increasing uniform attenuation ($\tilde{\eta}$) from an ensemble of two-port ($M = 2$) tetrahedral microwave graph data with broken TRI. The main figure shows a log-log plot of the PDF vs $|\mathrm{Im}[\tau_W]|$ for three values of uniform attenuation. A reference line is added to characterize the power-law tail. The inset shows the distributions of $\mathrm{Im}[\tau_W]$ on a linear scale for the same measured data.

Figure 1 demonstrates that the PDF of $\mathrm{Re}[\tau_W]$ exhibits power-law tails on both the negative and positive sides, respectively. The positive-side PDFs shown in Fig. 1 have different power-law behaviors for different ranges of $\mathrm{Re}[\tau_W]$, which is further explained theoretically in the Supplemental Material, Sec. II [45]. Figure 2 shows the PDF of $|\mathrm{Im}[\tau_W]|$ on both linear and log-log scales for the same values of uniform attenuation. We find that the $\mathrm{Im}[\tau_W]$ distribution is symmetric about zero to very good approximation. Once again a power-law behavior of the tails of the distribution is evident.

Figure 3 shows a plot of the Mean($\mathrm{Re}[\tau_W]$) vs uniform attenuation ($\tilde{\eta}$) in ensembles of microwave graphs for both

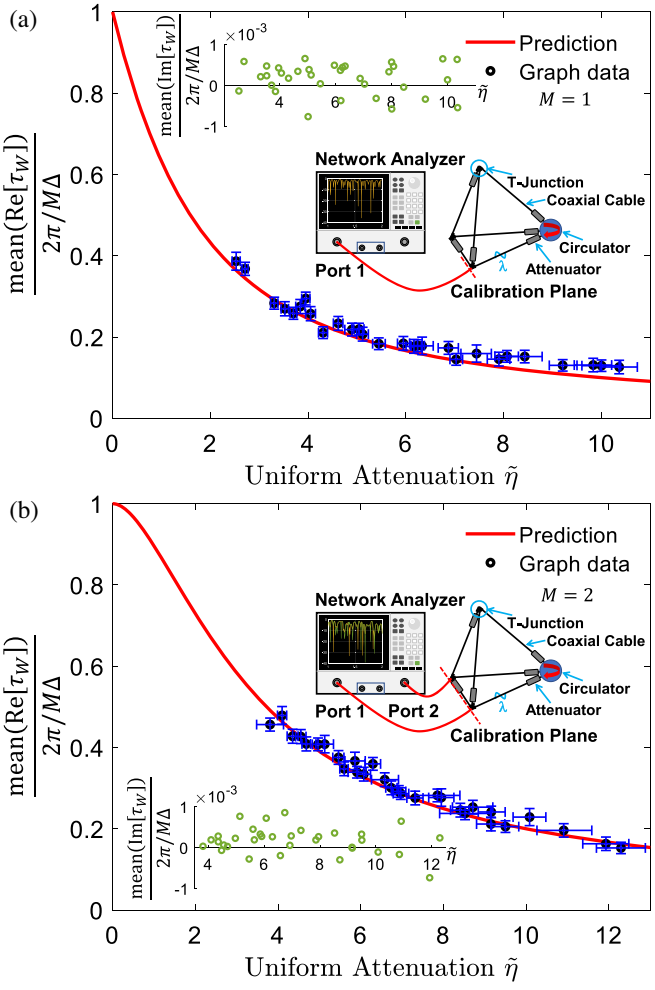

FIG. 3. Mean of $\mathrm{Re}[\tau_W]$ as a function of uniform attenuation $\tilde{\eta}$ evaluated using tetrahedral microwave graph data with broken TRI for both one- and two-port configurations. (a) One-port experimental data (black circles) compared with theory (red line). (b) Two-port experimental data (black circles) compared with theory (red line). A detailed discussion about the estimated error bars (blue) can be found in the Supplemental Material, Sec. V [45]. The insets show the mean of the $\mathrm{Im}[\tau_W]$ (green circles) as a function of uniform attenuation $\tilde{\eta}$ evaluated using the same datasets for the one- and two-port configurations, respectively. Other insets show the experimental configurations.

(a) $M = 1$ and (b) $M = 2$ ports. The black circles represent the data taken on an ensemble of microwave graphs with constant $\tilde{\eta}$. The red line is an evaluation of the relation Eq. (5), based on the analytical prediction for the $P(\Gamma_n)$ distribution for the (a) $M = 1$ and (b) $M = 2$ cases, both with perfect coupling ($g = 1$) [4,51]. Note that the distribution of Γ_n for $M = 1$ is very different from the multiports cases (see the Supplemental Material, Fig. S3 [45]). Nevertheless there is excellent agreement between data and theory over the entire experimentally accessible range of uniform attenuation values for both one-port and two-port graphs. We can conclude that the theoretical prediction put forward in Eq. (5) is in agreement with experimental data. A more detailed comparison with random matrix based computations over a broad range of uniform attenuation is presented in the Supplemental Material, Sec. IV [45].

We have also examined the experimentally obtained statistics of $\mathrm{Im}[\tau_W]$. As seen in the insets of Figs. 3(a) and 3(b), we find that the mean of $\mathrm{Im}[\tau_W]$ is consistent with theoretically predicted zero value for all levels of uniform attenuation in the graphs.

We now turn out attention back to the power-law tails for the distributions of $\mathrm{Re}[\tau_W]$ and $\mathrm{Im}[\tau_W]$ presented in Figs. 1 and 2. By examining the statistics of large values of $\mathrm{Re}[\tau_W]$ that appear in Eq. (3), one finds that the tails of the PDFs will behave as $\mathcal{P}(\mathrm{Re}[\tau_W]) \propto 1/\mathrm{Re}[\tau_W]^3$, on both the positive and negative sides, as long as $M\mathrm{Re}[\tau_W]/\tau_H \gg 1/\tilde{\eta}$ (details discussed in the Supplemental Material, Sec. II [45]). This behavior is clearly observed on the negative side of the PDF, as shown in Fig. 1(a). The tail on the positive side is more complicated due to a second power-law expected in the intermediate range: $\mathcal{P}(\mathrm{Re}[\tau_W]) \propto 1/\mathrm{Re}[\tau_W]^4$ when $1 \ll M\mathrm{Re}[\tau_W]/\tau_H \ll 1/\tilde{\eta}$. Unfortunately we were not able to obtain such data within this range (requiring very low attenuation $\tilde{\eta}$) experimentally, but a narrow range of $\mathrm{Re}[\tau_W]/\tau_H$ between approximately 0.3 and 1 in Fig. 1 shows a steeper power-law behavior, consistent with $\mathcal{P}(\mathrm{Re}[\tau_W]) \propto 1/\mathrm{Re}[\tau_W]^4$, giving way to a more shallow slope at larger values of $\mathrm{Re}[\tau_W]/\tau_H$, consistent with the theory. As seen in Fig. 2, the distribution of the imaginary part of the time delay has a wide range with a power law $\mathcal{P}(|\mathrm{Im}[\tau_W]|) \propto 1/|\mathrm{Im}[\tau_W]|^3$, consistent with our theoretical prediction.

Discussion.—We demonstrated that the CWTD is an experimentally accessible object sensitive to the statistics of S-matrix poles in the complex energy or frequency plane. In addition to the experimental results discussed above, we have also employed RMT, as well as associated numerical simulations, for studying the distribution of the CWTD. Through these simulations (Supplemental Material, Sec. IV [45]) we can explore much smaller, and much larger, values of uniform attenuation than can be achieved in the experiment. These simulations show agreement with all major predictions of the RMT-based theory, including the existence of an intermediate power law on the positive side of the $\mathcal{P}(\mathrm{Re}[\tau_W])$ distribution for low-loss systems. Finally we note that all results in Eqs. (1)–(5) are insensitive to the presence or absence of TRI. The power-law tail predictions are also insensitive to TRI, as shown in the Supplemental Material, Sec. II [45].

Conclusions.—We have experimentally verified the theoretical prediction that the mean value of the $\mathrm{Re}[\tau_W]$ for a system with uniform absorption strength η counts the fraction of scattering matrix poles with imaginary parts exceeding η. This opens a conceptually new opportunity to address resonance distributions experimentally, as we convincingly demonstrated with an ensemble of microwave graphs with either one or two scattering channels, and showing broken TRI and variable uniform attenuation. The tails of the distributions of both real and imaginary time delay are found to agree with theory.

We acknowledge Jen-Hao Yeh for early experimental work on complex time delay statistics. This work was supported by AFOSR COE Grant No. FA9550-15-1-0171 and ONR Grant No. N000141912481. Y. V. F. acknowledges financial support from EPSRC Grant No. EP/V002473/1.

*LChen95@umd.edu
†anlage@umd.edu
‡yan.fyodorov@kcl.ac.uk

[1] J. Verbaarschot, H. Weidenmüller, and M. Zirnbauer, Grassmann integration in stochastic quantum physics: The case of compound-nucleus scattering, Phys. Rep. **129**, 367 (1985).
[2] P. A. Mello, P. Pereyra, and T. H. Seligman, Information theory and statistical nuclear reactions. I. General theory and applications to few-channel problems, Ann. Phys. (N.Y.) **161**, 254 (1985).
[3] V. Sokolov and V. Zelevinsky, Dynamics and statistics of unstable quantum states, Nucl. Phys. **A504**, 562 (1989).
[4] Y. V. Fyodorov and H.-J. Sommers, Statistics of resonance poles, phase shifts and time delays in quantum chaotic scattering: Random matrix approach for systems with broken time-reversal invariance, J. Math. Phys. (N.Y.) **38**, 1918 (1997).
[5] Y. V. Fyodorov, D. V. Savin, and H.-J. Sommers, Scattering, reflection and impedance of waves in chaotic and disordered systems with absorption, J. Phys. A **38**, 10731 (2005).
[6] G. E. Mitchell, A. Richter, and H. A. Weidenmüller, Random matrices and chaos in nuclear physics: Nuclear reactions, Rev. Mod. Phys. **82**, 2845 (2010).
[7] Y. V. Fyodorov and D. V. Savin, Resonance scattering of waves in chaotic systems, in *The Oxford Handbook of Random Matrix Theory*, edited by G. Akemann, J. Baik, and P. D. Francesco (Oxford University Press, New York, 2011), pp. 703–722.
[8] A. Nock, S. Kumar, H.-J. Sommers, and T. Guhr, Distributions of off-diagonal scattering matrix elements: Exact results, Ann. Phys. (Amsterdam) **342**, 103 (2014).

[9] H. Schomerus, Random matrix approaches to open quantum systems, in *Stochastic Processes and Random Matrices: Lecture Notes of the Les Houches Summer School 2015*, edited by G. Schehr, A. Altland, Y. V. Fyodorov, N. O'Connell, and L. F. Cugliandolo (Oxford University Press, New York, 2017), pp. 409–473.
[10] D. G. Baranov, A. Krasnok, T. Shegai, A. Alù, and Y. Chong, Coherent perfect absorbers: Linear control of light with light, Nat. Rev. Mater. **2**, 17064 (2017).
[11] H. Li, S. Suwunnarat, R. Fleischmann, H. Schanz, and T. Kottos, Random Matrix Theory Approach to Chaotic Coherent Perfect Absorbers, Phys. Rev. Lett. **118**, 044101 (2017).
[12] Y. V. Fyodorov, S. Suwunnarat, and T. Kottos, Distribution of zeros of the *S*-matrix of chaotic cavities with localized losses and coherent perfect absorption: Non-perturbative results, J. Phys. A **50**, 30LT01 (2017).
[13] Y. V. Fyodorov, Reflection time difference as a probe of *S*-matrix zeroes in chaotic resonance scattering, Acta Phys. Pol. A **136**, 785 (2019).
[14] M. Osman and Y. V. Fyodorov, Chaotic scattering with localized losses: *S*-matrix zeros and reflection time difference for systems with broken time-reversal invariance, Phys. Rev. E **102**, 012202 (2020).
[15] L. Chen, S. M. Anlage, and Y. V. Fyodorov, Generalization of Wigner time delay to subunitary scattering systems, Phys. Rev. E **103**, L050203 (2021).
[16] E. P. Wigner, Lower limit for the energy derivative of the scattering phase shift, Phys. Rev. **98**, 145 (1955).
[17] F. T. Smith, Lifetime matrix in collision theory, Phys. Rev. **118**, 349 (1960).
[18] N. Lehmann, D. Savin, V. Sokolov, and H.-J. Sommers, Time delay correlations in chaotic scattering: Random matrix approach, Physica (Amsterdam) **86D**, 572 (1995).
[19] Y. V. Fyodorov and H.-J. Sommers, Parametric Correlations of Scattering Phase Shifts and Fluctuations of Delay Times in Few-Channel Chaotic Scattering, Phys. Rev. Lett. **76**, 4709 (1996).
[20] V. A. Gopar, P. A. Mello, and M. Büttiker, Mesoscopic Capacitors: A Statistical Analysis, Phys. Rev. Lett. **77**, 3005 (1996).
[21] Y. V. Fyodorov, D. V. Savin, and H.-J. Sommers, Parametric correlations of phase shifts and statistics of time delays in quantum chaotic scattering: Crossover between unitary and orthogonal symmetries, Phys. Rev. E **55**, R4857(R) (1997).
[22] P. W. Brouwer, K. M. Frahm, and C. W. J. Beenakker, Quantum Mechanical Time-Delay Matrix in Chaotic Scattering, Phys. Rev. Lett. **78**, 4737 (1997).
[23] P. W. Brouwer, K. Frahm, and C. W. J. Beenakker, Distribution of the quantum mechanical time-delay matrix for a chaotic cavity, Waves Random Media **9**, 91 (1999).
[24] D. V. Savin, Y. V. Fyodorov, and H.-J. Sommers, Reducing nonideal to ideal coupling in random matrix description of chaotic scattering: Application to the time-delay problem, Phys. Rev. E **63**, 035202(R) (2001).
[25] D. V. Savin and H.-J. Sommers, Delay times and reflection in chaotic cavities with absorption, Phys. Rev. E **68**, 036211 (2003).
[26] A. Ossipov and Y. V. Fyodorov, Statistics of delay times in mesoscopic systems as a manifestation of eigenfunction fluctuations, Phys. Rev. B **71**, 125133 (2005).
[27] T. Kottos, Statistics of resonances and delay times in random media: Beyond random matrix theory, J. Phys. A **38**, 10761 (2005).
[28] F. Mezzadri and N. J. Simm, Tau-function theory of chaotic quantum transport with $\beta = 1, 2, 4$, Commun. Math. Phys. **324**, 465 (2013).
[29] C. Texier and S. N. Majumdar, Wigner Time-Delay Distribution in Chaotic Cavities and Freezing Transition, Phys. Rev. Lett. **110**, 250602 (2013).
[30] F. D. Cunden, Statistical distribution of the Wigner–Smith time-delay matrix moments for chaotic cavities, Phys. Rev. E **91**, 060102(R) (2015).
[31] C. Texier, Wigner time delay and related concepts: Application to transport in coherent conductors, Physica (Amsterdam) **82E**, 16 (2016).
[32] A. Grabsch, Distribution of the Wigner-Smith time-delay matrix for chaotic cavities with absorption and coupled Coulomb gases, J. Phys. A **53**, 025202 (2020).
[33] J. Kuipers, D. V. Savin, and M. Sieber, Efficient semiclassical approach for time delays, New J. Phys. **16**, 123018 (2014).
[34] M. Novaes, Statistics of time delay and scattering correlation functions in chaotic systems. I. Random matrix theory, J. Math. Phys. (N.Y.) **56**, 062110 (2015).
[35] U. Smilansky, Delay-time distribution in the scattering of time-narrow wave packets. (I), J. Phys. A **50**, 215301 (2017).
[36] U. Smilansky and H. Schanz, Delay-time distribution in the scattering of time-narrow wave packets (II)—quantum graphs, J. Phys. A **51**, 075302 (2018).
[37] E. Doron, U. Smilansky, and A. Frenkel, Experimental Demonstration of Chaotic Scattering of Microwaves, Phys. Rev. Lett. **65**, 3072 (1990).
[38] A. Z. Genack, P. Sebbah, M. Stoytchev, and B. A. van Tiggelen, Statistics of Wave Dynamics in Random Media, Phys. Rev. Lett. **82**, 715 (1999).
[39] A. A. Chabanov, Z. Q. Zhang, and A. Z. Genack, Breakdown of Diffusion in Dynamics of Extended Waves in Mesoscopic Media, Phys. Rev. Lett. **90**, 203903 (2003).
[40] B. A. van Tiggelen, P. Sebbah, M. Stoytchev, and A. Z. Genack, Delay-time statistics for diffuse waves, Phys. Rev. E **59**, 7166 (1999).
[41] Y. Kang and A. Z. Genack, Transmission zeros with topological symmetry in complex systems, Phys. Rev. B **103**, L100201 (2021).
[42] V. Lyuboshitz, On collision duration in the presence of strong overlapping resonance levels, Phys. Lett. **72B**, 41 (1977).
[43] R. Pierrat, P. Ambichl, S. Gigan, A. Haber, R. Carminati, and S. Rotter, Invariance property of wave scattering through disordered media, Proc. Natl. Acad. Sci. U.S.A. **111**, 17765 (2014).
[44] U. Kuhl, O. Legrand, and F. Mortessagne, Microwave experiments using open chaotic cavities in the realm of the effective Hamiltonian formalism, Fortschr. Phys. **61**, 404 (2013).
[45] See Supplemental Material at http://link.aps.org/supplemental/10.1103/PhysRevLett.127.204101 for the details of proofs of Eq. (5) in the main text, discussions about the tails of the distribution functions of the complex Wigner

time delay, the sign convention used for the phase of the scattering matrix frequency evolution, further examination utilizing random matrix computations for the distribution functions of the complex Wigner time delay as a function of uniform attenuation, the attenuation value evaluation in the experiment as well as the error bars estimation in Fig. 3, and discussions and data about the TRI breaking effects produced by the circulator in the microwave graph. The Supplemental Material includes additional Refs. [46–49].

[46] Y. V. Fyodorov and M. Osman, Eigenfunction non-orthogonality factors and the shape of CPA-like dips in a single-channel reflection from lossy chaotic cavities, arXiv:2105.03665.

[47] S. D. Hemmady, A wave-chaotic approach to predicting and measuring electromagnetic field quantities in complicated enclosures, Ph.D thesis, University of Maryland, 2006, available at http://hdl.handle.net/1903/3979.

[48] F. Schäfer, Time-reversal symmetry breaking in quantum billiards, Ph.D thesis, Technische Universität Darmstadt, 2009, available at https://tuprints.ulb.tu-darmstadt.de/id/eprint/1329.

[49] P. So, S. M. Anlage, E. Ott, and R. N. Oerter, Wave Chaos Experiments with and without Time Reversal Symmetry: GUE and GOE Statistics, Phys. Rev. Lett. **74**, 2662 (1995).

[50] F. Haake, F. Izrailev, N. Lehmann, D. Saher, and H.-J. Sommers, Statistics of complex levels of random matrices for decaying systems, Z. Phys. B Condens. Matter **88**, 359 (1992).

[51] Y. V. Fyodorov and H. J. Sommers, Statistics of S-matrix poles in few-channel chaotic scattering: Crossover from isolated to overlapping resonances, JETP Lett. **63**, 1026 (1996).

[52] H.-J. Sommers, Y. V. Fyodorov, and M. Titov, *S*-matrix poles for chaotic quantum systems as eigenvalues of complex symmetric random matrices: From isolated to overlapping resonances, J. Phys. A **32**, L77 (1999).

[53] Y. V. Fyodorov and B. A. Khoruzhenko, Systematic Analytical Approach to Correlation Functions of Resonances in Quantum Chaotic Scattering, Phys. Rev. Lett. **83**, 65 (1999).

[54] U. Kuhl, R. Höhmann, J. Main, and H.-J. Stöckmann, Resonance Widths in Open Microwave Cavities Studied by Harmonic Inversion, Phys. Rev. Lett. **100**, 254101 (2008).

[55] A. Di Falco, T. F. Krauss, and A. Fratalocchi, Lifetime statistics of quantum chaos studied by a multiscale analysis, Appl. Phys. Lett. **100**, 184101 (2012).

[56] S. Barkhofen, T. Weich, A. Potzuweit, H.-J. Stöckmann, U. Kuhl, and M. Zworski, Experimental Observation of the Spectral Gap in Microwave *n*-Disk Systems, Phys. Rev. Lett. **110**, 164102 (2013).

[57] C. Liu, A. Di Falco, and A. Fratalocchi, Dicke Phase Transition with Multiple Superradiant States in Quantum Chaotic Resonators, Phys. Rev. X **4**, 021048 (2014).

[58] J.-B. Gros, U. Kuhl, O. Legrand, F. Mortessagne, E. Richalot, and D. V. Savin, Experimental Width Shift Distribution: A Test of Nonorthogonality for Local and Global Perturbations, Phys. Rev. Lett. **113**, 224101 (2014).

[59] M. Davy and A. Z. Genack, Selectively exciting quasinormal modes in open disordered systems, Nat. Commun. **9**, 4714 (2018).

[60] O. Hul, S. Bauch, P. Pakoński, N. Savytskyy, K. Życzkowski, and L. Sirko, Experimental simulation of quantum graphs by microwave networks, Phys. Rev. E **69**, 056205 (2004).

[61] M. Ławniczak, O. Hul, S. Bauch, P. Seba, and L. Sirko, Experimental and numerical investigation of the reflection coefficient and the distributions of Wigner's reaction matrix for irregular graphs with absorption, Phys. Rev. E **77**, 056210 (2008).

[62] O. Hul, M. Ławniczak, S. Bauch, A. Sawicki, M. Kuś, and L. Sirko, Are Scattering Properties of Graphs Uniquely Connected to Their Shapes?, Phys. Rev. Lett. **109**, 040402 (2012).

[63] L. Chen, T. Kottos, and S. M. Anlage, Perfect absorption in complex scattering systems with or without hidden symmetries, Nat. Commun. **11**, 5826 (2020).

[64] Z. Fu, T. Koch, T. M. Antonsen, E. Ott, and S. M. Anlage, Experimental study of quantum graphs with simple microwave networks: Non-universal features, Acta Phys. Pol. A **132**, 1655 (2017).

[65] B. Dietz, V. Yunko, M. Białous, S. Bauch, M. Ławniczak, and L. Sirko, Nonuniversality in the spectral properties of time-reversal-invariant microwave networks and quantum graphs, Phys. Rev. E **95**, 052202 (2017).

[66] The radiation S_{rad} is measured when the graph is replaced by 50 Ω loads connected to the three output connectors of each node attached to the network analyzer test cables.

[67] S. Hemmady, X. Zheng, E. Ott, T. M. Antonsen, and S. M. Anlage, Universal Impedance Fluctuations in Wave Chaotic Systems, Phys. Rev. Lett. **94**, 014102 (2005).

[68] X. Zheng, T. Antonsen, and E. Ott, Statistics of impedance and scattering matrices in chaotic microwave cavities: Single channel case, Electromagnetics **26**, 3 (2006).

[69] X. Zheng, T. M. Antonsen, and E. Ott, Statistics of impedance and scattering matrices of chaotic microwave cavities with multiple ports, Electromagnetics **26**, 37 (2006).

[70] G. Gradoni, J.-H. Yeh, B. Xiao, T. M. Antonsen, S. M. Anlage, and E. Ott, Predicting the statistics of wave transport through chaotic cavities by the random coupling model: A review and recent progress, Wave Motion **51**, 606 (2014).

[71] M. Ławniczak, S. Bauch, O. Hul, and L. Sirko, Experimental investigation of the enhancement factor for microwave irregular networks with preserved and broken time reversal symmetry in the presence of absorption, Phys. Rev. E **81**, 046204 (2010).

[72] M. Ławniczak and L. Sirko, Investigation of the diagonal elements of the wigners reaction matrix for networks with violated time reversal invariance, Sci. Rep. **9**, 5630 (2019).

[73] S. Hemmady, J. Hart, X. Zheng, T. M. Antonsen, E. Ott, and S. M. Anlage, Experimental test of universal conductance fluctuations by means of wave-chaotic microwave cavities, Phys. Rev. B **74**, 195326 (2006).